TELKOMNIKA, Vol. 11, No. 4, April 2013, pp. 2093~2101
ISSN: 2302-4046

Research on Flow Characteristics of Ultra-high Pressure Impinging Stream Micro-generator

LI Guang-ji*[1], LU Zheng-wen[2]
[1]School of Mechanical Engineering, Shanghai Institute of Technology, Shanghai 201418, China
[2]School of Economy and Management, Shanghai Institute of Technology, Shanghai 201418,China
*Corresponding author, e-mail: liguangji@126.com

Abstract

Design a new dynamic ultrahigh pressure structure in this article, this structure include three main zones. Simulate and analyze flow characteristics of three zones in details, providing the basis for the design of micro-size structure with ultra-high pressure. Liquid has gone through three broken and decentralized processes in micro-channels zone、impacting wall zone and flow impinging each other zone, find rule of mirror distribution in impinging zone. According to which, obtain the structure is reasonable. The fresh red wine is experimented, verifying that to obtain the same effect, dynamic ultrahigh pressure method greatly reduce energy consumption than ultra-static pressure. Further put forward and verifying a new method that is combining static and dynamic ultrahigh pressure method, can use a relatively lower pressure to get higher pressure treatment effect.

Keywords*: dynamic ultrahigh pressure, static ultrahigh pressure, flow characteristic, mirror distribution*

1. Introduction

In the present work a new dynamic ultrahigh pressure structure is studied. This structure make use of dynamic ultrahigh pressure technique that refers to the liquid mixtures direct to a predetermined pressure. Firstly, liquid mixtures flowing through the micro-channel, fluid can be refined, smash elementaryly in the micro-channel. Secondly, high-speed fluid fired at wall, the powerful impacting force from wall, ultrahigh pressure directly release, thus further bringing the material emulsion breaking and rapid sterilization. Thirdly, opposite flow of fluid collision result in a strong radial and axial turbulence velocity component, the role of a high degree of turbulence produce excellent mixed and dispersed in the impact zone.

Besides device structure designed, simulate the flow characteristics of three zones: micro-channel zone, impact wall zone and impinging against each other zone. These theoretical support for applying the structure, find new rules. The advantage of dynamic three zones of device structure act on emulsion breaking and rapid sterilization, to provide strong ultrahigh pressure technique are proved by experiments, which is to obtain the same effect with much lower than value of static ultrahigh pressure processing. Static ultrahigh pressure technique and dynamic ultrahigh pressure technique are two technologies used mainly to inactivate microorganisms or enzymes which damage fresh foods products. The advantage of using these novel technologies is that some of them are also called non-thermal technologies because the processing temperature does not rise beyond 40°C (Guerrero-Beltrán, Welti-Chanes, & Martín-Belloso, 2007). This is important to obtain Food-products with sensory and nutritional characteristics similar to fresh food products.

Static ultrahigh pressure approach is to put food to a particular ultrahigh pressure container, with water or liquid as a pressure medium, step-up to the set value, the static pressure to maintain a certain time, to gain processed food and germ killed. Static ultrahigh pressure technique was applied for the first time to treat foods, especially milk, by Hite (1899). First discovered 450MPa will extend the shelf-life of milk. Bridgman (1914) reported Protein can be solidified under 700MPa. Timson and Short (1965) treated raw milk using high pressure to reduce the microbial load. Since then, much research has been conducted using static ultrahigh pressure technique to accomplish several purposes, mainly microbial and enzyme inactivation. Nienaber and Shellhammer (2001) found Dp-values ranged from 4.6 to 117.5 min to inactivate pectinmethylesterase in orange juice treatedat pressures in the range of 400 to 600MPa.

Received January 13, 2013; Revised February 24, 2013; Accepted March 5, 2013

Research related to the effects of static ultrahigh pressure on vegetative microorganisms (Yuste, Capellas, Fung, & Mor-Mur, 2004), microbial spores (Estrada-Girón, Guerrero-Beltrán, Swanson, & Barbosa-Cánovas, 2007; Heinz & Knorr, 2001), and chemical reactions influencing quality (Ludikhuyze& Hendrickx, 2001) in fruit and vegetable products have been reported. activation or inactivation of food enzymes (Guerrero-Beltrán, Barbosa-Cánovas, & Swanson, 2004).

All of above-mentioned studies have been carried out using static ultrahigh pressure technique. Nevertheless, a few studies have been conducted using dynamic ultrahigh pressure technique for microbial or enzyme inactivation purposes. Device they used was homogenizer, for example, Taylor, Roach, Black, Davidson, and Harte (2007) observed a significant reduction of Escherichia coli K-12 in sodium chloride solutions (0.9%) in the range of 100 to 250MPa using a ultrahigh-pressure homogenizer. The aim of researches was to inactivate enzyme and natural microbial flora by dynamic ultrahigh pressure homogenization.

In this article, dynamic ultrahigh pressure technique use micro-channel, impacting to the wall and collision of two streams each other, experiment results analyze particle meters rather than enzyme inactivation.

The article is organized as follows. In Section 2 the formulation for giving the self-designed dynamic ultrahigh pressure structure and introduce process of refining and pulverization in key three zones. Next, Section 3 simulates and analyzes flow characteristic of three zones: micro-channel, micro-jet collide wall and impinge against each other, find rule of mirror distribution. Then fresh red wine is experimented separately by self-designed dynamic ultrahigh pressure structure and static ultrahigh pressure structure. Finally, section 4 summarizes the main contributions of the work.

2. Research Method

In this article we design a new dynamic ultrahigh pressure structure, this structure use advantages of the ultra-high pressure, impinging stream and micro-scale channel flow, liquid has gone through three broken and decentralized processes in which ultra-high pressure for the fluid to achieve very high speed provides the driving force.

Diameter of micro-channel is 0.1mm, not only enhanced mass transfer, and micro-channels were added to the friction and shear between liquid with wall, prior impacting a considerable portion of fluid can be refined, smash in the micro-tube. Micro-scale pipe can preserve high-voltage energy a greater extent the non-proliferation, result a high concentration of energy, energy loss. Fluid flow through the micro-tube is subjected to considerable shearing force.

After injection from the micro-tube, high-speed fluid fired at a fixed flat to create a strong impact force, the fluid is also given a powerful force from wall, the powerful impacting force from wall cause particles further broken and refined. In addition, because of large changes in velocity and pressure.

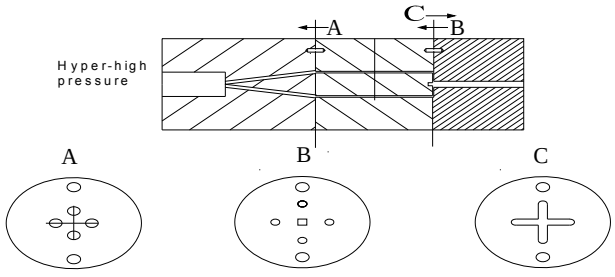

Figure 1. Structure of ultra-dynamic pressure impinging stream micro-generator

Changes cannot be ignored, the instant pressure change result in internal and external stress differences of droplet, in the role of internal and external stress difference, tensile stress is formed, to achieve ultrafine particles. Opposite flow of fluid collision result in a strong radial and axial turbulence velocity component, the role of a high degree of turbulence produce excellent mixed and dispersed in the impact zone.

3. Results and Analysis

3.1. Division of Micro Scale

We must first clarify the issue concerning the division of channel dimensions, now generally greater than 1mm is called macro-scale, lnm ~ 1mm is called micro-scale.

3.2. Study on Flow Characteristics of Micro-scale Tube

To establish the following coordinates, tube diameter is 0.1mm, length is 10mm, with water as the medium, 100MPa pressure on the import, export pressure with air-Linked.

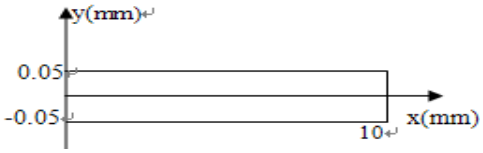

Figure 2. Coordinate System of Micro-scale Tube

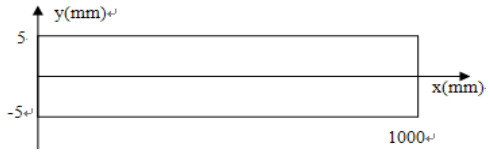

Figure 3. Coordinate System of Macro-scale Tube

As a contrast, at the same time simulate the flow characteristics of macro-pipe, establish the following coordinates, tube diameter is 10mm, length is 1000mm, with water as the medium, 100MPa pressure on the import, export pressure with air-Linked.

Figure 4 and Figure 5 respectively show velocity distribution at different locations in the direction of micro-scale tube and macro-scale tube pipe, y= 0 is central axis, There is a acceleration process after water into the tube which diameter is 0.1 millimeter, the speed of the largest can reach 448m/s. While water flow into the tube which diameter is 10 millimeter, the speed of the largest reach only 317m/s. Without the absence of the driving role of outside pressure, energy loss, velocities are declining, velocity of micro-pipe had a little drop and reach 446m/s, velocity of macro-scale tube has declined to reach 313m/s, remained stable until to export.

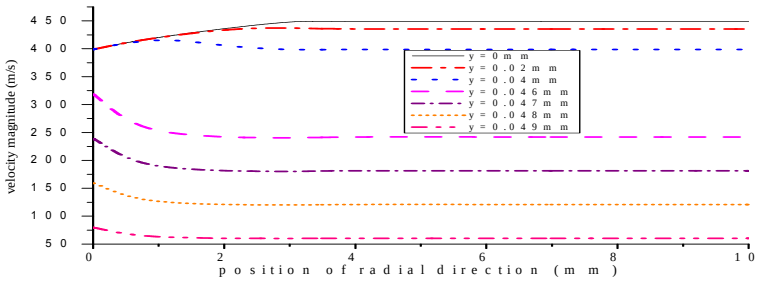

Figure 4. Velocity Distribution in Different Locations along Radial Direction of Micro-size Tube (diameter is 0.1mm, length is 10mm)

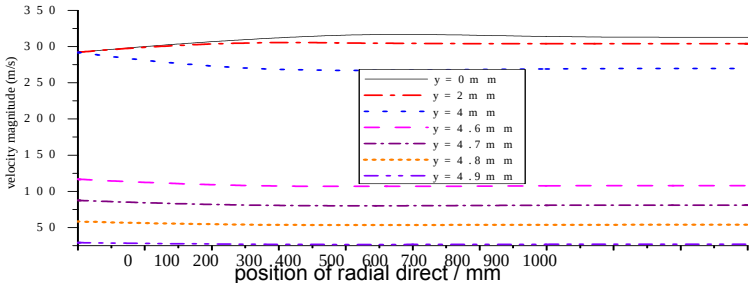

Figure 5. Velocity Distribution in Different Locations along Radial Direction of Macro-size Tube (diameter is 10mm, length is 1000mm)

Analysis and comparison of two Figures can conclude axis velocity variation tendency in the micro-scale pipe is consistent with in macro-scale. Under the same driving pressure, pipe diameter sizes from micro-scale 0.1millimeter to macro-scale 10 millimeter, speed is reduced, that is, in micro-scale tube the axis velocity is larger 130 m/s than in macro-scale pipe, micro-scale pipe can uttermost preserve the energy of the non-proliferation and preserve high degree of energy concentration. along the y = 0.046mm, 0.047mm, 0.048mm, 0.049mm order gradually close to the border. It can be seen from the Figure the variety trend is consistent in micro-scale tube and macro-scale tube, velocity in micro-scale pipe is larger 100m/s-120m/s than in the macro-scale tube.

Figure 6 and Figure 7 respectively show wall shearing stress distribution at different locations in the y direction of micro-scale tube and macro-scale tube pipe, only near to wall there is shearing stress, the shearing stress is 4.2 times in the micro-scale tube than in the macro-scale pipe. Fluid is suffered from very large shearing force through the micro-tube, a considerable portion of fluid in micro-tube can be refined, crushed.

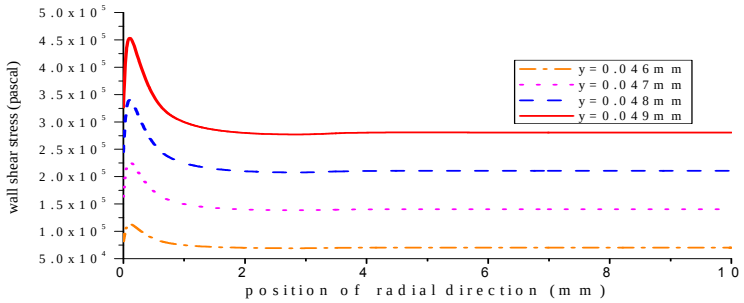

Figure 6. Shearing Force Distribution of Micro-scale Tube at Different Locations in the Radial Direction (diameter is 0.1mm, length is 10mm)

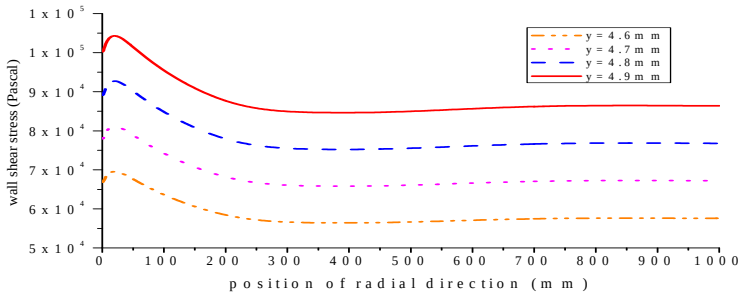

Figure 7. Shearing Force Distribution of Macro-scale Tube at Different Locations in the Radial Direction (diameter is 10mm, length is 1000mm

3.3. Prediction of the Impact of Ejected Flow on the Wall

In this work, standard $k-\varepsilon$, RNG $k-\varepsilon$, Realizable $k-\varepsilon$ models are applied to numerically simulate the impact of ejected flow on wall. Predicted values will be compared to the experimental data for evaluation and further improvement of the models. Figure 8 is structure of ejected flow on wall.

Three models including standard *k-ε*, RNG *k-ε*, and Realizable models, are used to simulate the fluid flow on two planes, y/b=1 and y/b=4, after it is ejected from the micro-generator, and impacts on the wall. The predictions are compared to experimental values (S.Ashforth—Frost, and K. Jambunathan, 1996)

Figure 9 shows the simulated distributions of average velocity and turbulent flow strength on y/b=1 plane from the three models. As shown in (a), axial velocity distribution calculated from the k-ε standard model fits the experimental data close to the wall better, but the error increases gradually away from the wall. However, RNG model (Yonghong Liu, Xiantao Wang, Masahiro Takei. 2013) fits the experimental data better than standard k-ε model in

general, except in the limited area close to the wall where larger error occurs. Realizable model gives the best prediction.

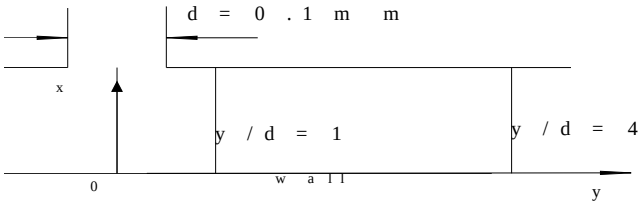

Figure 8. Structure of Ejected Flow on Wall

Comparing to the experimental results both in trend and predicted values. (b) shows similar features that Realizable model gives the best fit to experimental data, RNG is the second best, and standard k- ε model the last.

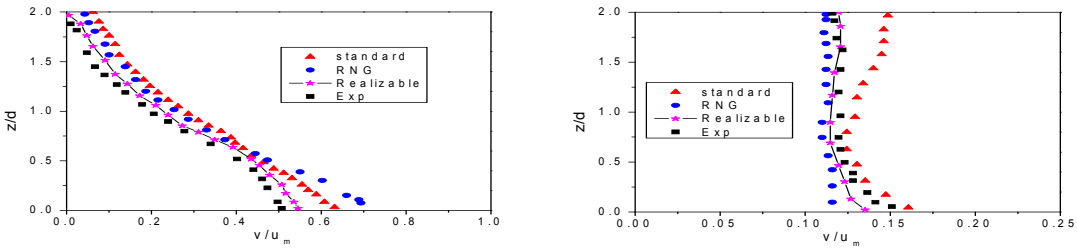

(a) Average velocity distribution and (b) Turbulent Flow Strength Distribution

Figure 9. Distributions of average velocity and turbulent flow strength on y/b=1 plane

Figure 10 shows the predictions of average velocity and turbulence strength distributions on y/b=4 plane from the three models. In general, predictions on y/b=1 plane from the three models fit experimental data better than those on y/b=4 plane. For instance, larger error occurs on y/b=4 plane from standard k- model; on y/b=4 plane from RNG K- model, although prediction is in agreement with experimental result, comparatively, Realizable model fits experiment result the best both in trend and prediction.

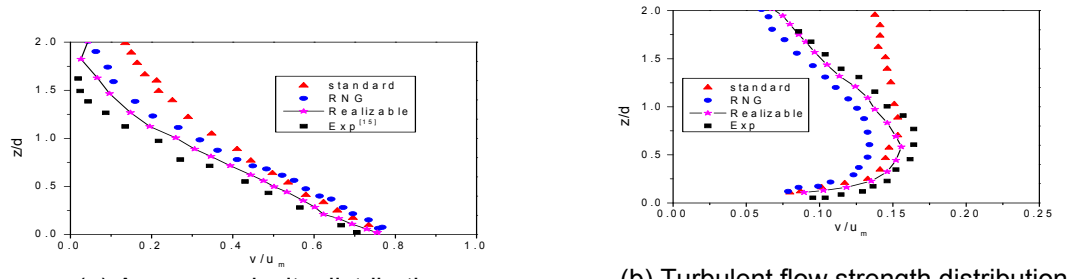

(a) Average velocity distribution (b) Turbulent flow strength distribution

Figure 10. Distributions of Average Velocity and Turbulent Flow Strength on y/b=4 Plane

In summary, through the comparison between the experimental data and simulations of average velocity and turbulence strength on y/b=1 and y/b=4 planes, it can be concluded. That realizable model fits the experiment result the best, RNG model the next, and standard k- ε model the worst.

3.4. Flow Characteristics of Impinging Flow

Impact flow is very complex, so far studies on the phenomenon are not sufficient. Powell (1960) proposed a mirror-model (Nosseir N, Pelet U, Hildebrand G,1968; Denshchikov V A, Kontratev, V N, Romashov A V,1978) with two ejected flow with a distance of S collide on the plane located at the middle distance. In other words, impact wall is the mirror plane for everything in the impact area. Regarding the turbulence flow, no reference clarify that everything in the impact area is on mirror symmetry to the impact plane. In this work, impact flow with a super-high pressure, 300MPa is studied. No reference indicates whether it belongs to mirror-model. The coordinate is established as Figure 11:

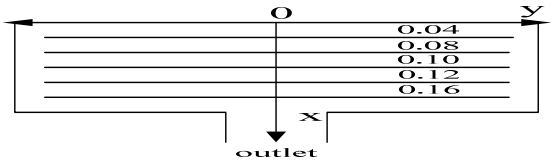

Figure 11. Coordinate of the Model

In Figure 12 and Figure 13, velocity on y axis keeps constant from the beginning until close to the impact plane, and drops rapidly to zero (on impact plane, y=0) where the axial velocity of the fluid turns into zero. Velocity in x axis is completely the opposite. From the beginning, it is almost zero and increases gradually close to the impact plane until reaching the maximum where the axial velocity. Changes into the radial speed.

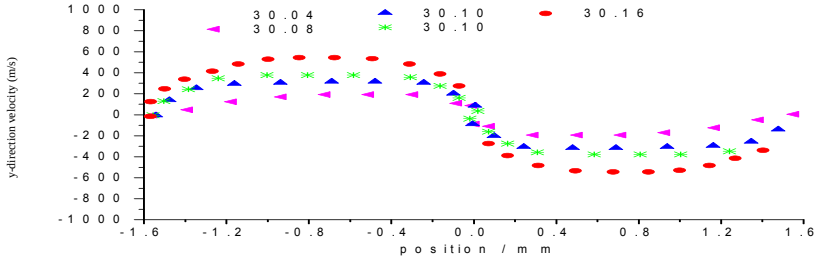

Figure 12. Y-direction Velocity of 5 Sections in Impinging Zone

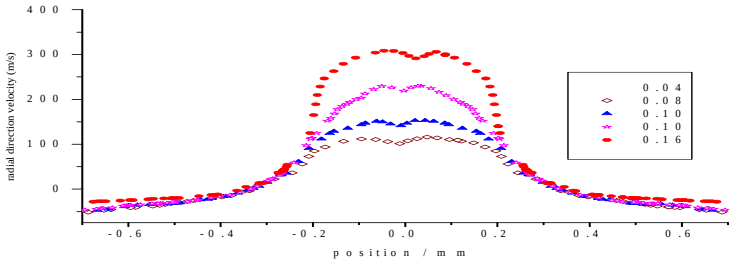

Figure 13. X-direction Velocity of Five Sections in Impinging Zone

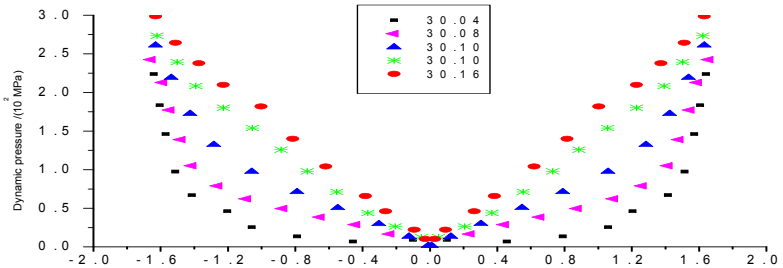

Figure 14. Dynamic Pressure Diagram of 5 Sections in Impinging Zone

Figure 14 shows the two flows are mostly symmetrical to the impact plane, and the dynamic pressures of the flows in y direction reduce gradually to zero at the impact plane, dynamic transform kinetic energy, because the kinetic energy is proportional to the velocity. When the fluid flows towards the impact plane, the x-direction velocity attains a maximum value at the impact plane.

3.5. Experiment

Analytical instrument: Ultra-violet spectral analysis instrument. Experimental material: Fresh red grape wine. Experimental method (Xiaopeng Li, Hao Guo, Jingnian Liu, Yali Liu 2013). Static ultrahigh pressure method and dynamic ultrahigh pressure method were used to process wine. Dynamic ultrahigh pressure process method: From the bottle to take a certain amount of wine into the of dynamic ultrahigh pressure impinging stream micro-generator, a direct step-up to 150MPa, wine samples processed directly for the determination.

UV absorption spectra of wine determination: The sample was determined by ultraviolet spectral analysis instrument, absorption cell capacity 100μl, wavelength scanning range 200-600nm, scanning speed fast, wavelength scanning units: 1nm.

The Figure x-coordinate is the scanning wavelength (nm), y-coordinate is the absorbance (ABS). From the Figure 20 It can be seen that fresh wine is gone through ultrahigh pressure, wine-like shape of the spectrum, a peak number, position and absorption intensity peaks have changed.

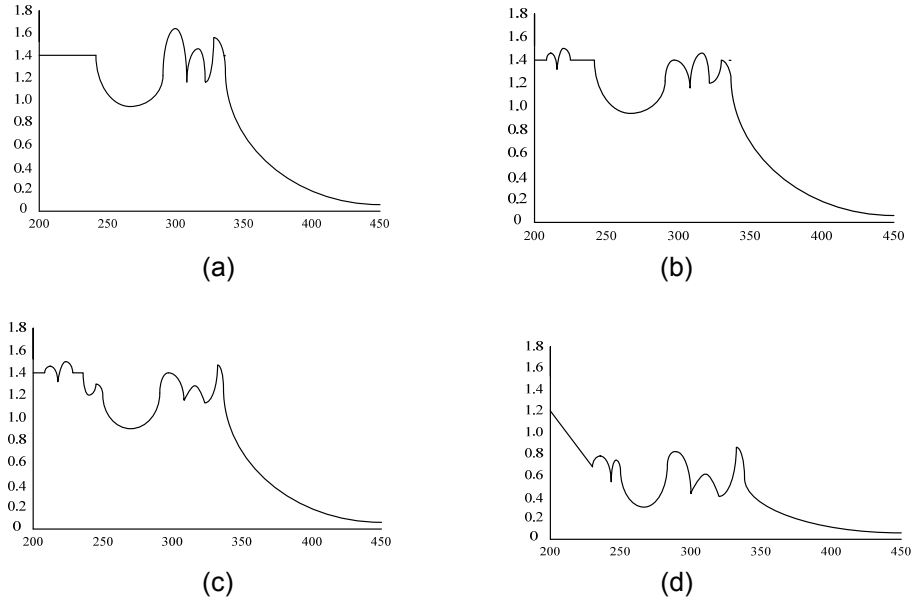

Figure 15. (a) Ultraviolet absorption line of raw wine and; (b) ultraviolet absorption line of 200MPa static pressure and; (c) ultraviolet absorption line of 150MPa dynamic pressure and; (d) ultraviolet absorption line of methods of dynamic pressure and static pressure.

Figure 15(a) is UV absorption spectral curve of the original liquor: ABS of the original wine is 1.4 absorption line at a wavelength of 200-230nm, four strong absorption peaks are at a wavelength of 250-350nm. Figure 15(b) is UV absorption spectrum after 200MPa static ultrahigh pressure treatment, there is a level line of absorption values 1.4 at a wavelength of between 200-230nm , but the straight-line distance become shorter, in the middle there are two very narrow peaks. At the wavelength 250-350nm intensity of 4 absorption peaks are reduced, and curve is slightly flat.

Figure 15(c) is UV absorption spectral curve by 150MPa dynamic pressure treatment, the shape of Figure 15(c) and Figure 15(b) is closer, the only difference is at a wavelength of 240nm there is a weak absorption peak, which can be verified that to obtain the same effect, dynamic ultrahigh pressure method greatly reduce energy consumption than ultra-static pressure. Figure 15(d) is UV absorption spectral curve of combining the two methods, first

handled by static ultrahigh pressure then dynamic ultrahigh pressure, the absorption of horizontal lines between wavelength of 200-230nm is broken, horizontal line become slash, between wavelength of 230-240nm there are the two relatively weak peaks, the absorption intensity is smaller, between wavelength of 250-350nm shape of four peaks has changed little compared to the preceding Figures, but the absorption intensity is smaller.

Graphic changes can be explained as follows: under ultrahigh pressure volume of wine decreases with increase of pressure. The distance between molecules in the wine has been compressed, alcohol molecules and water molecules are re-arranged. External pressure provide the part of the energy that association require, to break the original natural conditions of water and alcohol combination of state, the promotion of association reaction.

A variety of substances in wine such as organic acids, aldehydes, ketones, aromatic organic compounds at 200-400nm near-ultraviolet region have the maximum absorption, wine handled by 200MPa static ultrahigh pressure treatment cause polymerization between certain elements of the wine, making the location、conformation of groups and absorb wavelengths there are changes. Treatment effect by 150MPa dynamic ultrahigh pressure is equivalent to treatment effect by 200MPa static ultrahigh pressure.

Alone in a method, taking into account the pump performance problems, when the pressure attains 350MPa, it is difficult to further increase , combining static and dynamic ultrahigh pressure method could be considered ,so that we can use a relatively low pressure to get high pressure treatment effect. Figure 15(d) indicated spectral curve with 150MPa static pressure processing, then with 200MPa dynamic pressure processing. Analyzing variation trends in spectral curve, equivalent to treatment results with only static pressure method or dynamic pressure method that greater than 200MPa. Figure 15(d) confirm the feasibility of combining static and dynamic ultrahigh pressure method.

This change of curve is because, when the pressure continues to increase, some material is unbearable to the pressure force, pressure relief cannot recovery original spatial structure, such as protein denaturation condensation, tannin, anthocyanin polymer molecules, so that pigment content decreased, absorption wavelength and absorption values have changed.

4. Conclusion

This article integrate the impinging stream and micro-scale generator to ultrahigh pressure technologies and make use of the advantages of three to design a new, efficient, durable, subminiature structure. the following deserve to be highlighted:

1. Micro-scale tube preservation of high-voltage energy of the non-proliferation and contain the energy highly concentrated than macro-scale tube, a considerable portion of fluid can be refined, smash in the micro-tube.
2. Three models including standard *k-ε*, RNG *k-ε*, and Realizable models, are used to simulate the fluid flow on two planes that is y/b=1 and y/b=4 after it is ejected from the micro-generator, and impacts on the wall. Realizable model gives the best fit to experimental data, RNG is the second best, and standard k-*ε* model the last.
3. In the impinging zone, new rule was found that velocities in x and y directions, dynamic pressure are symmetrical to the impact plane.
4. The fresh red wine is experimented separately by self-designed dynamic ultrahigh pressure structure and static ultrahigh pressure structure, verifying that to obtain the same effect, dynamic ultrahigh pressure method greatly reduce energy consumption than ultra-static pressure. Further put forward and verifying a new method that is combining static and dynamic ultrahigh pressure method, we can use a relatively low pressure to get high pressure treatment effect. We believe that it can be of considerable value in the areas of structure design, simulation analysis and experiment. For future work, we plan to use other materials to experimentally validate the structure.

Aknowledgement

This work was supported by the National Natural Science Foundation of China (Grant No.51205257), the Shanghai Institute of Technology (Grant No.YJ2011-19)

References

[1] Guerrero-Beltrán JA, Welti-Chanes J, Martín-Belloso O. *Pulsed electric fields processing of peach nectar to inactivate polyphenoloxidase*. Institute of Food Technologists annual meeting and food expo. Chicago, USA. 2007.

[2] Hite BH. The effects of pressure in the preservation of milk. Bull of the West Virginia Univ. Agricultural Experimental Station. 1899; 58: 16–35.

[3] Timson WJ, Short AJ. Resistance of microorganisms to hydrostatic pressure. *Biotechnology and Bioengineering*. 1965; 7: 139–159.

[4] Nienaber U, Shellhammer TH. High-pressure processing of orange juice: Kinetic of pectinmethylesterase inactivation. *Journal of Food Science.* 2001; 66(2): 328–331.

[5] Yuste J, Capellas M, Fung DYC, Mor-Mur M. Inactivation and sublethal injury of foodborne pathogens by high pressure processing: evaluation with conventional media and thin agar layer method. *Food Research International*. 2004; 37: 861–866.

[6] Estrada-Girón Y, Guerrero-Beltrán JA, Swanson BG, Barbosa-Cánovas GV. Effect of high hydrostatic pressure on spores of Geobacillus stearothermophilus suspended in soymilk. *Journal of Food Processing and Preservation* .2007; 16: 194–203.

[7] Heinz V, Knorr D. *Effects of high pressure on spores*. In M. E. G. Hendrickx & D. Knorr (Eds.), Ultra high pressure treatments of foods. New York, USA: Klumer Academic/Plenum Publishers. 2001; 77-113.

[8] Ludikhuyze L, Hendrickx MEG. *Effects of high pressure on chemical reactions related to food quality*. In M. E. G. Hendrickx & D. Knorr (Eds.), Ultra high pressure treatments of foods. NewYork, USA: Klumer Academic/Plenum Publishers. 2001; 167–188.

[9] Ludikhuyze L, Van Leoy A, Indrawati Denys S, Hendrickx MEG. *Effects of high pressure on enzymes related to food quality*. In M. E. G. Hendrickx & D. Knorr (Eds.), Ultra high pressure treatments of foods. New York, USA: Klumer Academic/Plenum Publishers. 2001; 115–166.

[10] Guerrero-Beltrán JA, Barbosa-Cánovas GV, Swanson BG. High hydrostatic pressure processing of peach puree with and without antibrowning agents. *Journal of Food Processing Preservation*. 2004; 28: 69–85.

[11] Taylor TM, Roach A, Black DG, Davidson PM, Harte F. Inactivation of Escherichia coli K-12 exposed to pressures in excess of 300 MPa in a high-pressure homogenizer. *Journal of Food Protection*. 2007; 70(4): 1007–1010.

[12] S Ashforth Frost, K Jambunathan. Numerical prediction of semi—confined jet impingement and comparison with experimental data. *Int JNum erMethodsinFluids*. 1996; 23: 295-306.

[13] Powell A. Aerodynamic noise and the plane boundary. *J Acoustical Society of America*. 1960; 32: 982-990.

[14] Nosseir N, Pelet U, Hildebrand G. Pressure field generated by jet on jet impingement. *AIChE J*.1968; 25: 78-84.

[15] Denshchikov VA, Kontratev VN, Romashov AV. Interaction between two oppesed jets. *Fluid Dynamics*.1978; 6: 924-926.

[16] Yonghong Liu, Xiantao Wang, Masahiro Takei. Solid-Liquid Two-Phase Flow Image Reconstruction Based on ERT Technique in Microchannel. *Telkomnika Indonesian Journal of Electrical Engineering.* 2013; 11(1).

[17] Xiaopeng Li, Hao Guo, Jingnian Liu, Yali Liu. Dynamical Characteristics of the Linear Rolling Guide with Numerical Simulation and Experiment. *Telkomnika Indonesian Journal of Electrical Engineering*. 2013; 11(1).